FULL PAPER

Convergent Modeling Strategies to Account for SAR on 3-aminopyridazines Binding to m₁ Muscarinic Receptor

Nicolas Thevenin, Philippe Bernard, Hélène Bourdon, Marcel Hibert, and Camille-Georges Wermuth

Laboratoire de Pharmacochimie de la Communication Cellulaire, UMR CNRS/ULP 7081, Faculté de Pharmacie, 74 route du Rhin, F-67400 Illkirch-Graffenstaden, France. Tel: +33-388 676818; Fax: +33-3 88 674794; E-mail: mhibert@pharma.u-strasbg.fr

Abstract The binding mode of 3-aminopyridazine analogues to the M1 muscarinic receptor has been studied by two complementary modeling strategies: the "active analog" approach and direct docking into a 3D model of the receptor. Modeling combined with SAR study: (i) accounts for the contribution to binding of both hydrophilic (Asp311, Asn617) and hydrophobic residues; (ii) illustrates the subtlety of ligand-receptor binding; (iii) highlights a binding site domain that might be responsible to partial or full agonism.

Keywords G-Protein-Coupled Receptors, Ligand-based alignment, Protein-based alignment

Introduction

The five identified muscarinic receptors (m_1-m_5) are members of the superfamily of membrane-bound receptors that regulate cellular activity *via* coupling to heterotrimeric G-proteins. [1, 2] These muscarinic receptors are found in different areas of the brain and in the periphery, and are involved in many different physiological processes. The binding site for acetylcholine and several agonists and antagonists on muscarinic receptors is located within the seven transmembrane helices which are characteristic of all G-protein-coupled receptors (GPCRs). [1, 3, 4] Agonists and antagonists able to discriminate receptor subtypes represent valuable pharmacological tools and potentially useful therapeutic agents. Particularly, m_1-selective agonists may be

useful to enhance cognitive functions in Alzheimer-patients as Alzheimer's disease (AD) is associated with a deficit in cholinergic activity. [5] In addition, it has been recently shown that the activation of the m_1 receptors would be involved in the non amyloidogenic pathway which would be beneficial in the treatment of AD. [6]

In order to rationalize the search for new muscarinic ligands, the ligand-based approach led us to propose pharmacophoric patterns for muscarinic ligands. [7, 8] As soon as the m_1 receptor sequence became available, three-dimensional models based on both bacteriorhodopsin and rhodopsin structures were built. [3, 9] During the search for central cholinergic agents that do not induce the cholinergic syndrome, we managed to improve, using classical structure-activity relationship (SAR) studies, the affinity of the partial agonist minaprine for the hippocampic muscarinic m_1 receptor by a factor of 5660 [10] (Table 1, compounds **1-4**). Critical improvements resulted from a shift of the 4-methyl group to the 5-position, replacement of morpholine

Correspondence to: M. Hibert

by a more lipophilic amine and introduction of a phenolic hydroxyl in *ortho* position of the 6-phenyl ring.

Aiming at rationalizing these results, we performed a molecular modeling study of 3-aminopyridazines and a selection of other partial and full muscarinic agonists using the "active analog" approach, and subsequently, we examined their possible docking mode to the binding site of the recently refined 3-D model of the muscarinic m1 receptor. [11] The two modeling strategies are presented and discussed.

Experimental procedure

Modeling was performed on a Silicon Graphics workstation O2 R10000 with the commercially available SYBYL 6.4 software package. [12]

Ligand molecular modeling

Besides the 3-aminopyridazines **1** to **4**, we also studied a bridged analog, compound **5**, as well as the non-pyridazine full agonists **9** to **11**, **13** and **18**, and the partial agonists **6** to **8, 12, 14** to **17**. All structures and biological data are presented in Table 1. [10, 11, 13-17] The distinction between partial and full agonist properties is based on the ability of the compound tested to modulate the concentration of inositol phosphate, compared to the full agonist carbachol compound. [16] The 18 ligands were modeled as follows. The starting conformations of each compound were optimized by molecular mechanics using the Tripos force field. [18] The Sybyl/Systematic search option, with an angle step of 30° for the search, was used to explore the conformational space of each ligand. All conformers generated were then submitted to energy minimization using the Tripos force field with a convergence criterion of 0.01 kcal/mol. The AM1 semiempirical method [19] was used to calculate the electrostatic term.

For the pharmacophore/ligand-based alignment, the putative bioactive conformation was selected by means of the root mean square (RMS) option of Sybyl (see below).

For the protein-based alignment of each compound, the selected putative bioactive conformation was used as initial conformation for docking.

Pharmacophore/ligand-based alignment

The pharmacophoric pattern for muscarinic m_1 agonists was used to identify the putative active conformation of each compound. For that purpose, we fitted all conformers generated for each compound on the oxadiazole (compound **10**, Table 1) which was already used as a template in our former study. [11] In this study, we showed that the atom of protonated nitrogen in the piperidine ring of compound **10**, corresponding to the ammonium of acetylcholine, interacts with Asp311 by an electrostatic interaction. We also noticed a putative

hydrogen bond between Asn617 and the oxygen atom in the oxadiazole ring of **10**, corresponding to the carbonyl of acetylcholine. These two atoms of compound **10** were defined as superimposition points to establish the structure-based alignment of the 17 compounds. The C5 atom of the oxadiazole ring was defined as the third point, which allows us to adjust the orientation of the oxygen electronic ion pairs. These three atoms were used to evaluate the RMS value for all conformers of each ligand. This value was calculated by means of the "Fit Atoms" option of Sybyl and the best RMS value was used to define the bioactive conformation of each ligand.

For each ligand, the three homologous atoms to the oxiadazole reference were defined as follows: (i) All the cationic nitrogen atoms were fitted on the protonated atom of compound **10**. (ii) The choice of the two others atoms was more delicate because, in some cases, several solutions were found. For example, since compound **13** possesses two carbonyl groups, two structural alignments with the oxadiazole reference were investigated. Thus, for each conformer of this compound **13**, two RMS values were calculated and the better allowed to select the bioactive conformation.

Protein-based alignment

The active conformations selected above were docked in the binding cleft of the refined 3-D model of the muscarinic m_1 receptor. [11]

Actually, this new model was optimized starting from the model published by Hibert *et al*, [3] in order to obtain an optimal fit with the bovine rhodopsin footprint published by Schertler. [20] Furthermore, the N-terminal end of the receptor, the three extracellular loops and the first and second intracellular loops were also added to the refined model, which was then submitted to a molecular dynamics simulation with a constraint on the backbone, allowing the side chains to adjust. The same simulation was then repeated without the constraint on the backbone. The molecular dynamics simulation was performed at constant temperature with an integration step of 0.5 fs. The structure of the receptor was initialized at 300 °K starting from a Boltzmann distribution set followed by 200 ps of simulation, also at 300 °K. The conformations were recorded every 200 fs. The Tripos force field was used with the Kollman charges [21] as electrostatic contribution. A dielectric constant equal to 1 was applied.

In order to select the best model, a statistical evaluation of all the recorded conformations was performed using the Verify 3D algorithm [22] by means of the Verify 3D structure evaluation server (www.doe-mbi.ucla.edu/services/verify3D.html). The conformation giving the best 3D/1D scores was selected as our muscarinic m_1 receptor model.

Finally, the model was subjected to energy minimization using the Tripos force field with a convergence criterion of 0.01 kcal mol^{-1}. The Kollman charges were still used as electrostatic contribution.

Conformers extracted from the superimposition of the agonists were separately and manually docked in the puta-

tive binding site. The residues involved in the ligand-receptor interactions have been described in our previous article [11]: they have been characterized by molecular modeling, site-directed mutagenesis experiments, and sequence homology analysis (Figure1). Thus, we tried to conserve the ion pair between the positive ammonium of the ligand and Asp311 located on helix 3. [23] Then, we considered Asn617 located on helix 6 for which the mutation to Ala was shown to decrease the affinity of agonists and antagonists [24] in the m_1 and m_2 subtypes, while it had no effect in the m_3 subtype. [25]

All of the complexes obtained by manual docking were subjected to a dynamics study. which allows the relative positioning of each residues surrounding the ligand and the adjustment of the anchor fragment around its position. The molecular dynamics studies, applied to each complex, were performed at constant temperature with an integration step of 0.5 fs and a coupling of 50 fs. The structures were initialized at 300 °K starting from a Boltzmann distribution set followed by 200 ps of simulation at the same temperature. The conformations were recorded every 100 fs. The molecular dynamics procedure was only applied to the ligand and the residues around this ligand within a radius of 8 Å. The Tripos force field was used with the Kollman charges for the protein and the AM1 charges for the ligand. A dielectric constant equal to 1 was applied. The average structure was selected as valid structure for each model. The complexes were finally minimized. An approximation of the binding energy E_{int} resulting from the ligand binding into the protein was calculated as follow:

$$E_{int} = E_{complex} - (E_{receptor} + E_{ligand})$$

Where $E_{complex}$, $E_{receptor}$ and E_{ligand} are the energies of the complex, the receptor and the ligand, respectively. This approximate evaluation does not take the solvation energy into account.

Results and discussion

Pharmacophore/ligand-based alignment

For each of the agonists superimposed on the reference molecule, oxadiazole, it was possible to find a stable conformation (energy difference never higher than 5 kcal mol^{-1} above the global minimum), which allowed an excellent superimposition between the three selected atoms of the oxadiazole reference and three atoms of each ligand (Figure 2). When a compound gave several possible alignment profiles, all of them were tested. Indeed, compound **13**, for example, gives four solutions because of the presence of both two carbonyl groups and two conformers of the piperidine ring. Four different RMS values were calculated (0.2, 0.4, 0.7 and 0.95) and the conformation with the lowest RMS value was considered as the selected conformer.

Fitting the 3-aminopyridazines on the oxadiazole reference molecule led us to the three following observations: (i) between the two pyridazinic nitrogens, the N2 nitrogen, which is assumed to correspond to the carbonyl oxygen atom of acetylcholine, achieves the best fit to the oxygen atom of the oxadiazole reference molecule (Figure 2a). This finding will be compared to the docking assays described below. (ii) The second observation concerns all the considered partial agonists: interestingly, it appears that the phenyl ring common to all the partial agonists is located in the same spatial area (Figure 2b). This additional hydrophobic area could represent a fourth pharmacophoric element that apparently induces a partial agonist profile in a non-restrictive way (arecoline or milameline for instance, which are also partial agonists, do not have such an aromatic ring). Figure 2b indicates in yellow the distances between the different pharmacophoric elements. (iii) The last observation concerns the two isomers **8** and **9**, which do not have the same functional activity profile. Indeed, the oxime **8** behaves as a partial agonist, whereas the oxime **9** is a full agonist. On the superimposition view of these two compounds (Figure 2c), we can notice that, due to the double bond isomerism change, the phenyl ring of the *cis* isomer (compound **9**) cannot be located in the same area as the phenyl ring of the *trans* isomer (compound **8**) and that of all other partial agonists. This suggests a different binding mode of the two isomers that might confer the partial or full agonist property. In fact, all the better conformers of compound **9** are able to form an intramolecular π-cation interaction between the ammonium group and the phenyl ring, with a conformational energy gain of about 5 to 10 kcal mol^{-1}
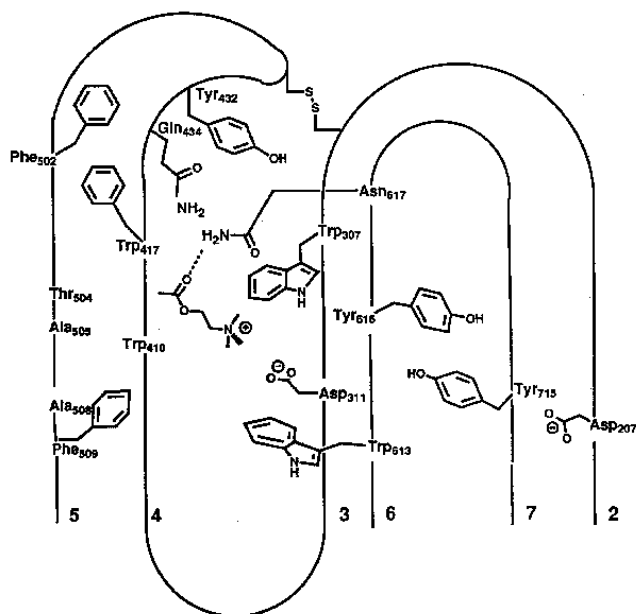

Figure 1 *Schematic representation of the active site of the refined 3D-model of the muscarinic m_1 receptor*

compared to the others conformers. Due to the stereochemistry, this conformation is not possible in compound **8**.

In a previous article, the pharmacophoric pattern of other centrally acting muscarinic ligands was described [8]. Superimpositions of muscarinic agonists and antagonists were performed using the active analog approach. It was noticed that the phenyl ring of minaprine or its analogs was located in a region of space which does not induce antagonist properties. Interestingly, this is also true for the partial agonists **6** to **8**. In addition, the aromatic ring of the full agonist compound **9** occupies neither the putative partial agonist domain nor the antagonism domain already defined [8].
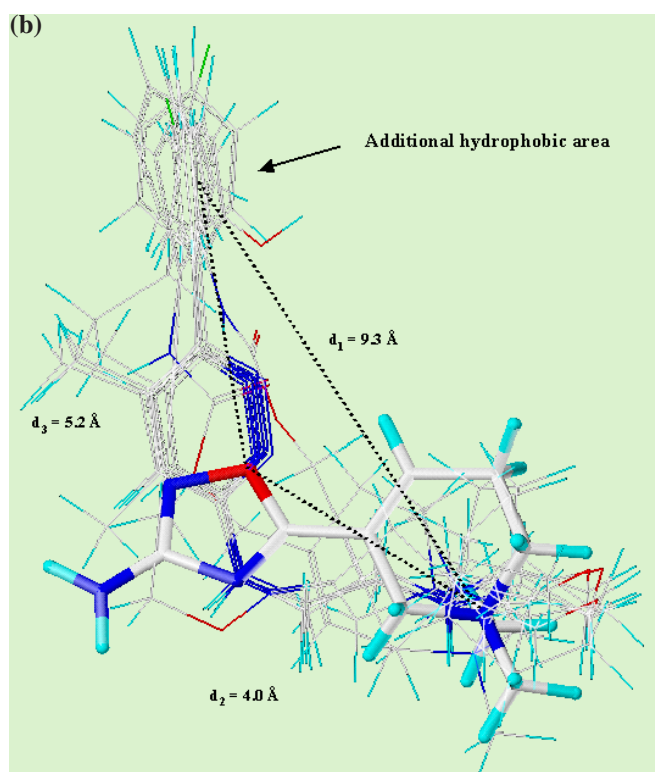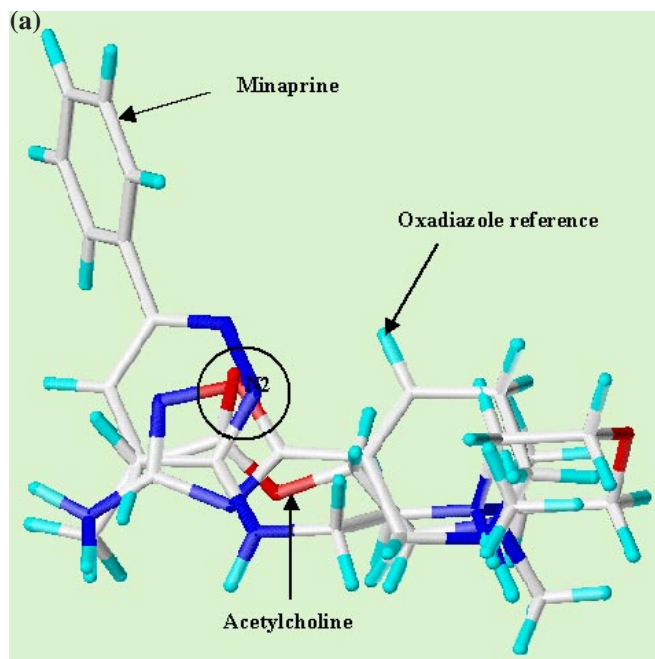
Protein-based alignment

In order to rationalize the increase in affinity observed during the chemical modifications made on minaprine and to investigate the binding mode of the studied compounds, we fitted each of them in the binding site of the refined 3-D model of the m_1 muscarinic receptor. This binding site consists mainly of a pocket surrounded by helices 3, 4, 5, 6 and 7. Docking the active conformations of the minaprine analogues revealed the following interesting points :

(i): The protein-based approach suggests an interaction of N1, rather than N2, of the pyridazine ring with the residue Asn617, although the active analog approach (Figure 2a) revealed a better fit between the N2 nitrogen atom and the oxygen atom of compound **10**. Moreover, the active analog approach result was in agreement with the fact than N2 is more basic than N1 in such aromatic systems. [26] This docking result could be explain by the fact that an hydrogen bond
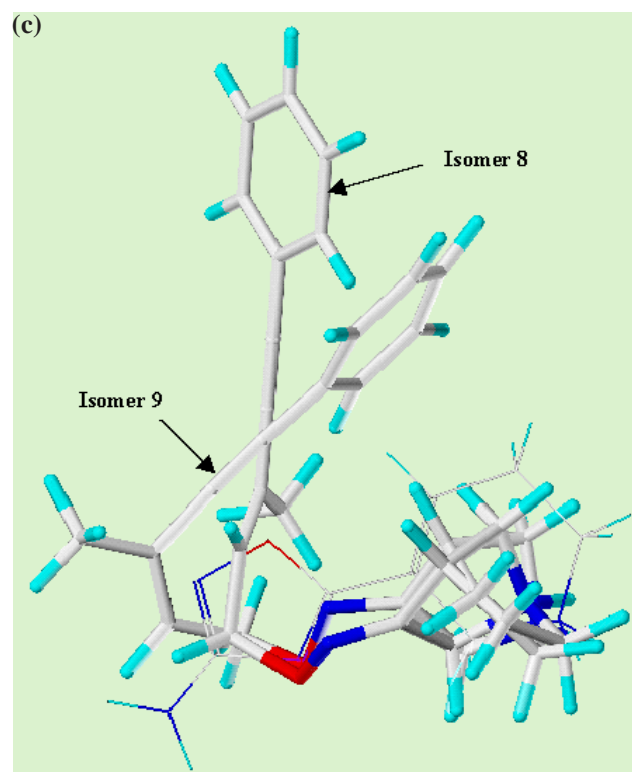
Figure 2 *Ligand-based alignment of (**a**) minaprine and acetylcholine on the oxadiazole reference, (**b**) compounds **1** to **8** on the oxadiazole reference and (**c**) compounds **8** and **9** on the oxadiazole reference*
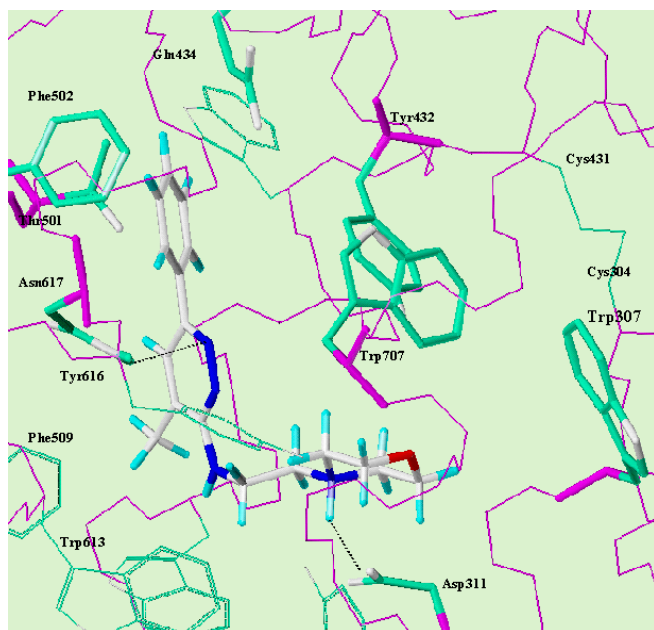
Figure 3 *Docking of minaprine. The electrostatic interactions are indicated in black*

between N2 and Asn617 in the receptor model would generate a worse ionic interaction by taking away the morpholine nitrogen and Asp311. Consequently, N1 is better located than N2 to establish a H-bond with Asn617 (Figure 3). This observation is in agreement with earlier SAR studies, from which it was concluded that an optimal basicity of the N1 nitrogen atom was essential for the affinity. In these studies, the H4 hydrogen atom of the pyridazine ring was systematically replaced by different groups. It appeared clear that an electron donor group such as methyl, ethyl, phenyl, benzyl, CH$_2$-β-naphtyl improves binding, whereas electron withdrawing substituents showed lower binding data compounds. [27]

(ii) In the refined model of the m$_1$ receptor, as observed in the other GPCR models based on bovine rhodopsin projection map, [4] the binding cleft is wider than in bacteriorhodopsin. It possesses an extra aromatic environment located near the extracellular side between helices 3, 4 and 5 and composed of residues Trp417, Tyr432 and Phe502. The side chain positions of these residues has already been described as being modified by the aromatic ring of the docked partial agonist **7**. [9] The observation we made from the docking of compounds **1** to **8** confirmed that, in the active conformations of all these partial agonists, the phenyl ring can establish π-π interactions with the residues Trp417, Tyr432 and Phe502 of the above mentioned aromatic environment (Figures 3 to 5). These aromatic interactions have the usual geometry of neighboring aromatic groups of peptides or proteins, *i.e.* a distance <7 Å between the phenyl rings centroids and a dihedral angle between the phenyl rings planes around 50°. [28] Besides establishing a hydrogen bond with Asn617 *via* its carbonyl oxygen (like McN-A-343), compound **6**, can localize its phenyl ring in this aromatic domain. However,

due to their different structures, the two isomers **8** and **9** cannot establish the same local interactions with the binding cleft of the receptor (Figure 4). Actually, the *trans* isomer, which behaves as a partial agonist, can bind to the active site of the m$_1$ receptor in a very similar way to the other partial agonists. It can form a hydrogen bond with Asn617 *via* the oxygen atom of its oxime moiety and establish aromatic interactions with Trp417, Tyr432 and Phe502 (Figure 4). On the contrary, the more folded structure of the *cis* isomer, which behaves as a full agonist, prevents it from interacting with all residues of the above-mentioned aromatic pocket but allows it to preferentially interact with the aromatic ring of Trp307, Tyr432 and Trp707, which means closer to the active site of full agonists (Figure 4). Another argument in favor of this alignment concerns the docking. Indeed, the docking of compound **9** reveals a binding energy of –70 kcal·mol^{-1} in its folded structure whereas the same compound aligned like compound **8** possesses a worse binding energy of –55 kcal·mol^{-1}. In this last solution, the interaction with Asn617 is lost.

We also tried to understand the differences in affinity observed by the chemical modifications introduced on minaprine. The first observation was the increase in the affinity by a factor of 30 when moving the methyl substituent of the pyridazine ring from the 4 to the 5 position. A possible explanation had to be found preferentially in the conformation of the ligand itself. To what extent can the methyl group shift from the 4- to the 5-position affect the conformation of the whole molecule ? We could have assumed that the dihedral angle σ (Table 1) constrained by steric hindrance of the methyl in the 4-position imposed a particular conformation on the molecule, which could not be obtained by moving the
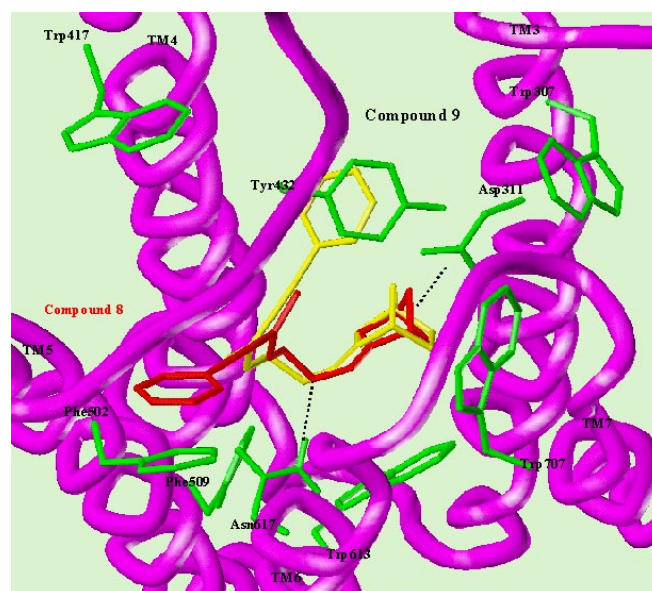
Figure 4 *Docking of compounds **8** in red and **9** in yellow. This protein-based alignment is different compared to the ligand-based alignment shown in Figure 2c*

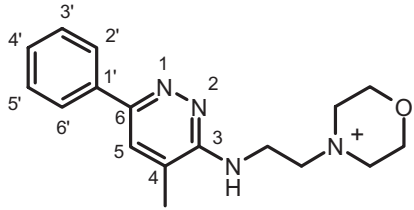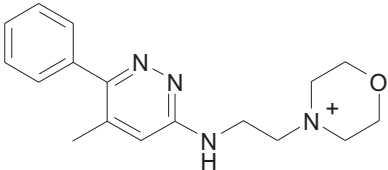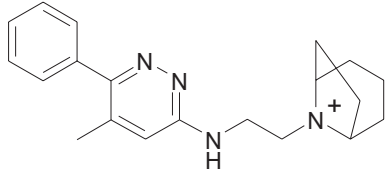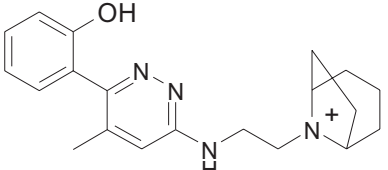**Table 1** *Biological activity of the studied m₁ muscarinic agonists*
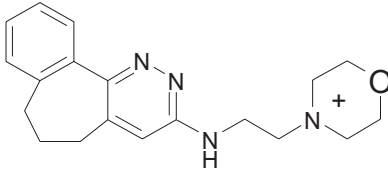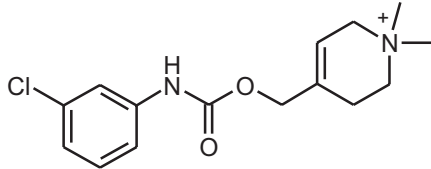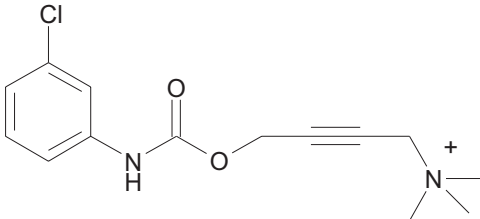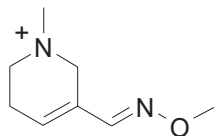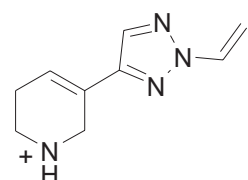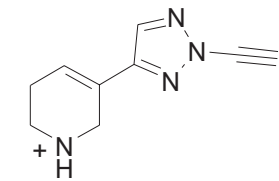
Cpnd	Name	Structure	Activity type	Activity
1	Minaprine		Partial agonist [10]	17000[a]
2	3-(morpholino-2 ethylamino)-5-methyl-6-phenyl-pyridazine		Partial agonist [10]	550[a]
3	3-(nortropano-2 ethylamino)-5-methyl-6-phenyl-pyridazine		Partial agonist [10]	60[a]
4	3-(nortropano-2 ethylamino)-5-methyl-6-orthohydroxy-phenyl-pyridazine		Partial agonist [10]	3[a]
5	3-(morpholino-2 ethylamino)-dihydro-6,7-5*H* benzocyclohepta [5,6-*c*] pyridazine		Partial agonist [10]	370[a]
6	Isoarecolinol phenyl carbamate		Partial agonist [11]	0.1 - 0.3[b]
7	McNeil-A-343		Partial agonist [11]	955[a]

Table 1 *Continued*

Cpnd	Name	Structure	Activity type	Activity
8	Azabicyclooxime Parke-Davis *trans*		Partial agonist [7]	12.4[c]
9	Azabicyclooxime Parke-Davis *cis*		Full agonist [7]	0.15[c]
10	Tetrahydropyridyl-oxadiazole		Full agonist [11]	0.0017[d]
11	Talsaclidine (WAL 2014)		Full agonist [13]	235[e]
12	Xanomeline		Partial agonist [14]	7[e]
13	RS 86		Full agonist [15]	490[e]
14	Oxotremorine		Partial agonist [11]	65[e]
15	Sabcomeline (SB 202026)		Partial agonist [15]	10[e]

Table 1 *Continued*

Cpnd	Name	Structure	Activity type	Activity
16	Milameline		Partial agonist [16]	1 100[e]
17	2-allyl-4-(3-piperidyl)-1,2,3-triazole		Partial agonist [17]	100[e]
18	4-(3-piperidyl)-2-propargyl-1,2,3-triazole		Full agonist [17]	84[e]

[a] IC_{50} (nM), [³H] pirenzepine (rat hippocampic m_1 receptor)
[b] increase in mean blood pressure (mmol/kg i.v., rat)
[c] IC_{50} (nM), RCMD

[d] Kapp mM, [³H] oxotremorine-M (rat brain membrane)
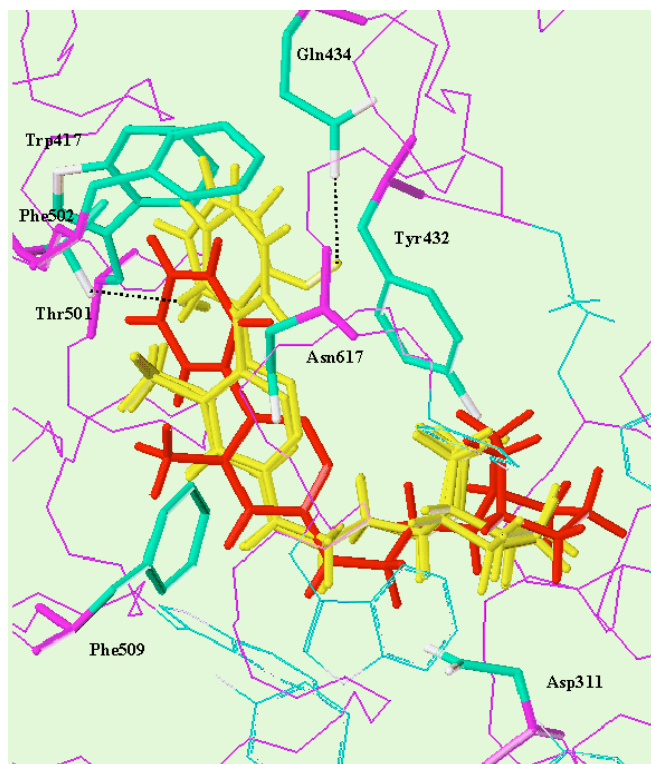[e] Ki (nM), [³H] pirenzepine (cloned m_1 receptor in A9 L cells); fφ: dihedral angle N1-C6-C1'-C2'; σσ: dihedral angle N(exocyclic)-C3-C4-Methyl

methyl group to the 5-position. However, X-ray structures of aminopyridazines available from the Cambridge Structural Database [29-31] show that the dihedral angle σ always lies around 180°, whatever the 4 substituent is. This is due to the steric hindrance of the 4-substituent, which forces the side chain to point toward the opposite side. This position remains stable due to the electronic delocalization between the *exo*-amidinic nitrogen atom and the pyridazine ring, which provides a π character to the exocyclic N-C bond. While the dihedral angle σ was not changed by displacement of the methyl group, on the contrary, the free rotation of the phenyl ring at the other side of the molecule was affected. Crystallographic data on the aminopyridazines [29] have also shown that the length of the bond C_6-C_1, was characteristic of a simple bond, which means that there is no delocalization between the two aromatic rings. In the case of the 4-methyl compound (minaprine, compound **1**), the phenyl ring is totally free to rotate, but in the case of the 5-methyl compound (compound **2**), the rotation of the phenyl ring is prevented to a certain extent by the steric hindrance due to the closer methyl group. We evaluated these geometric and steric features by performing a systematic search with an increment of 5° on the rotatable bond between the phenyl and pyridazine rings of both minaprine and 5-methyl minaprine. Indeed, in the case of minaprine, we obtained more low energy conformations than in the case of 5-methyl minaprine. This means that

the phenyl ring rotates more freely in the case of minaprine, which does not favor the active conformation of the whole molecule. More particularly, the global minimum of 5-methyl minaprine corresponds to a value of 55° for the dihedral angle φ (Table 1), which is consistent with the value of 51° of the crystal structure [31] and which is also close to the value of this angle (50°) in the docked conformation.

In summary, the pyridazine nucleus being anchored in the binding site as described above, the phenyl ring of aminopyridazines is found docked with some aromatic residues (Trp417, Tyr432 and Phe502) located at the top of the binding site (*i.e.* a dihedral angle φ of approximately 50°). This orientation is imposed by a favorable geometry of interaction between the phenyl ring of the ligand and the aromatic rings of Trp417, Tyr432 and Phe502 and by the steric hindrance with some neighboring residues. Furthermore, this selected conformation is close to the global minimum (energy difference = 1 to 5 kcal mol⁻¹) and is favored when the rotation of the phenyl ring is more constrained by the methyl substituent in the 5-position. Another argument supporting this hypothesis is afforded by compound **5**. In this molecule, the relative position of the phenyl ring is completely fixed to a dihedral angle φ of 40° (which is close to 50°) by a three carbon atom bridge. Interestingly, this compound possesses an affinity similar to compound **2** (5-methyl minaprine) for the m_1 receptor (IC_{50} = 0.37 mM and 0.55 mM, respectively).

Figure 5 *Docking of compounds 3 in red and 4 in yellow. The two possible docking of compound 4 are shown. The hydrogen bonds are indicated in black*

aromatic residues (Phe509, Trp613, Trp307 and Trp410), which could form a stabilizing π-cation complex.

The final improvement in the affinity of minaprine analogues was achieved by substitution of one of the *ortho* hydrogens of the phenyl ring by an hydroxyl group. Interestingly, the model suggests that this hydroxyl moiety is able to form two hydrogen bonds with Gln434 located in the second extracellular loop on one hand and Thr501 on helix 5 (Figure 5) on the other hand. Both residues are conserved among the muscarinic receptor subtypes. Gln434 has already been proposed to contribute to pilocarpine anchoring in the human m_1 muscarinic receptor in a previous study. [11] According to mutagenesis results reported by Wess *et al* on the m_3 receptor, [33] Thr501 could also play a role in the binding of muscarinic agonists. The lower flexibility of the phenyl ring induced by the *ortho* hydroxyl group next to the methyl group, together with the two additional hydrogen bonds made by this moiety, may be responsible for the excellent affinity of this compound compared to minaprine.

Convergence of the two approaches

In this study, we characterized the putative binding mode of pyridazine muscarinic partial agonists using two different but complementary approaches: the first one was an indirect method, *i. e.* the active analog approach, which allowed us to refine our pharmacophore model for muscarinic agonists. This indirect approach also led us to make a hypothesis about the identity of the pyridazinic nitrogen capable of establishing a hydrogen bond with a polar residue of the binding site. The second approach was a more direct one, *i. e.* the docking of the compounds in a model of the receptor. Comparing these two methods, we can conclude that the first one gives access to the pharmacophore and the main characteristics of the binding site, while the second one allows us to refine the analysis. Indeed, two points were refined by the protein-based approach: (i) the identity of the pyridazinic nitrogen atom preferentially involved in a hydrogen bond was not supported by the structure-based approach and (ii) the docking of com-

Docking of aminopyridazines in the m_1 receptor also allowed us to check the hypothesis we made from structure-activity-relationships, concerning the lipophilic environment of the cationic head. Indeed, replacing the morpholino group of the cationic head by a nortropane moiety increased the affinity by a factor of 9. This is not surprising when we observe that, as already described, [32] the ion pair formed by the ammonium and Asp311 is surrounded by some conserved
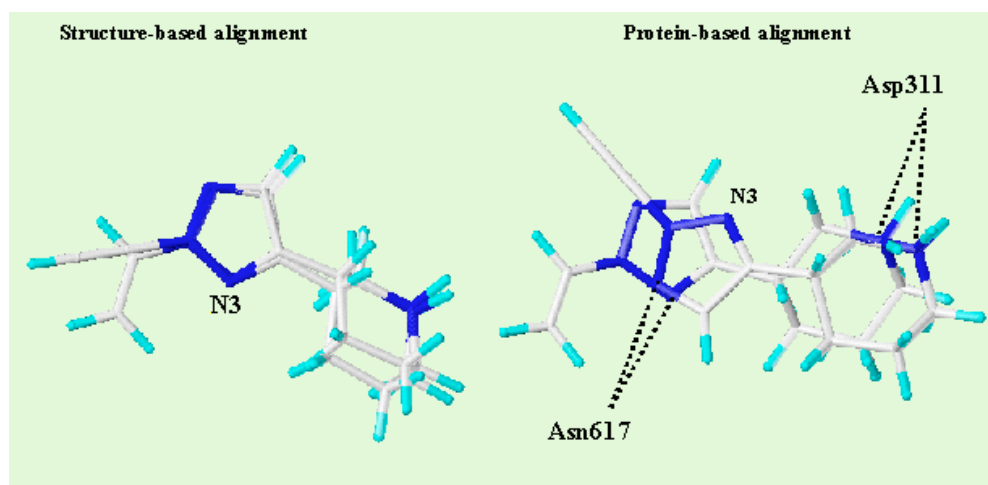
Figure 6 *Structure-based alignment of compounds 17 and 18, compared to their protein-based alignment*

pounds **17** and **18** reveals a protein-based alignment different than the structure-based alignment (Figure 6). Indeed, in the structure-based alignment, the best fit corresponds to the alignment of the triazol nitrogen atoms of compounds **17** and **18**, with those of the reference oxadiazole compound. This structure-based alignment is verified by docking for compound **17**, which interacts with Asp311 and Asn617. This alignment allows the positioning of its allyl group near the helix 5 of the receptor, towards the cavity defining the putative partial agonist activity. In such a conformation, the binding energy of the ligand is about –50 kcal mol^{-1}. Another conformation of compound **17** is found, consisting in the rotation of 180° of its triazol ring, but with a worse binding energy of –43 kcal mol^{-1}. Concerning compound **18**, which also interacts with Asp311 and Asn617, its less flexible propargyl group generates a steric hindrance with the helix 5. In this conformation, the hydrogen bond between Asn617 and the compound is lost. Thus, considering that compound **18** is anchored by its ammonium group, a rotation of 180° around its flexible bond linking the two rings, is observed in the docked complex. In this conformation, Asn617 interacts with one other triazol nitrogen atom, N1 rather than N3. Therefore, the propargyl group is directed towards the residues Trp307 and Tyr432, already found to interact with the phenyl ring of compound **9**. Interestingly, this compound possesses the same full activity profile as compound **18**. Finally, although the new conformational energy of compound **18** is slightly lower (about 1.5 kcal mol^{-1}) than this found in the structural alignment, the binding energy resulting from the docking is better by about 6 kcal mol^{-1}; this difference being explained by the presence or absence of the Asn617-compound hydrogen bond.

However, more general features proposed by the first approach could be validated by the second one. As an example, the aromatic residues suggested by the superimposition of the phenyl ring of all the considered partial agonists did exist in the binding site of the refined model of the m$_1$ receptor. Furthermore, it was proposed by a similar indirect approach [8] that the phenyl ring of minaprine or its analogs is located in a region which does not induce antagonistic properties. In our previous article, we showed that antagonist activity of tricyclic compounds requires aromatic interactions not only with the aromatic region located at the top of the binding cleft, but also with some aromatic residues (Trp410, Tyr613) located at the bottom of the agonist binding site. [11] Interestingly, we also observed that the antagonistic activity of NMS, which possesses only one phenyl ring, seemed to be due to the aromatic interactions it makes with the bottom of the binding site (with residues Trp410 and Tyr613). This reinforces the hypothesis according to which lipophilic interactions with the top of the binding cleft would confer partial agonist activity and that antagonists properties would be mainly induced by aromatic interactions with the bottom of the binding site. Finally, the three dimensional model of the receptor allowed to suggest some additional interactions (hydrogen bonds of the hydroxyl function of compound **4** with residues Gln434 and Thr501) that were suggested by the first approach.

Conclusion

Ligand-based and docking studies of the 3-amino-6-arylpyridazines **1** to **4** seem to allow the rationalization, in the limit of each of these strategies, of the favorable effects on potency and efficacy resulting from empirical SAR studies. All the minaprine analogs could make an ionic pair between the cationic head and Asp311, as well as a H-bond between probably the N1 pyridazinic nitrogen and the Asn617 residue on helix 6. An aromatic region (composed of residues Trp417, Tyr432 and Phe502) was found to be located ideally to accommodate the phenyl ring of the 6-arylpyridazines and other compounds that possess the same partial agonist profile.

The increase in affinity observed as a result of the chemical modifications introduced on minaprine could be explained by :

- a stabilization of the active conformation of the molecule : the shift of the methyl group from the 4- to the 5-position (compound **1** to **2**) constrained the rotation of the phenyl ring, optimizing the interaction with the above-mentioned aromatic residue cluster.

- an increase in the lipophilicity of the cationic head, which is surrounded by a lipophilic cage of aromatic residues in the receptor (compound **2** to **3**),

- an additional interaction points with the Thr501 and Gln 434 residues (compound **3** to **4**).

In order to confirm this model, additional experiments are now necessary, such as mutagenesis and site directed photoaffinity-labeling. Actually, some other synthetic minaprine analogues are being tested in order to validate these results as well as evaluation of other relevant minaprine analogs.

References

1. Nathanson, N. M. *Annu. Rev. Neurosci.* **1987**, *10*, 195.
2. Hulme, E. C.; Birdsall, N. J. M.; Buckley, N. J. *Annu. Rev. Pharmacol. Toxicol.* **1990**, *30*, 633.
3. Hibert, M.; Trumpp-Kallmeyer, S.; Bruinvels, A.; Hoflack, *J. Mol. Pharmacol.* **1991**, *40*, 8.
4. Baldwin J. M. *EMBO J.* **1993**, *12*, 1693.
5. Sims, N. R.; Bowen, D. M.; Allen, S. J.; Smith, C. C. T.; Neary, D.; Thomas, D. J.; Davidson, A. N. *J. Neurochem.* **1983**, *40*, 503.
6. Fisher, A; Brandeis, R; Haring, R; Eshhar, N; Heldman, E.; Karton, Y. *et al*. *J. Physiology (Paris)* **1998**, *92*, 337.
7. Bourdon, H. *Modélisation des modes d'interaction de ligands muscariniques avec le modèle tridimensionnel du recepteur M1. Application aux 3-aminopyridazines*, Louis Pasteur University of Strasbourg, France, 1995, PhD Thesis.
8. Hoffmann, R.; Bourguignon, J. J.; Wermuth, C. G. In Silipo, S. and Vittoria, A. (Eds) *QSAR : Rational approaches to the design of bioactive compounds*, Elsevier Science Publishers B. V; Amsterdam, 1991, pp. 283-292.
9. Nordvall, G.; Hacksell, U. *J. Med. Chem.* **1993**, *36*, 967.

10. Wermuth, C. G. *Il Farmaco* **1993**, *48*, 253.
11. Bourdon, H.; Trumpp-Kallmeyer, S.; Schreuder, H.; Hoflack, J.; Hibert, M.; Wermuth, C. G. *J. Comput-Aided Mol. Design* **1997**, *11*, 317.
12. Sybyl 6.4 is available from Tripos Associates, 1699 South Hanley Road, St Louis, MO 63144.
13. Walland, A.; Burkard, S.; Hammer, R.; Tröger, W. *Life Sciences* **1997**, *60*, 977.
14. Wood, M. D.; Murkitt, K. L.; Ho, M.; Watson, J. M.; Brown, F.; Hunter, A. J.; Middlemiss, D. N. *Br. J. Pharmacol.* **1999**, *126*, 1620.
15. Hodges, H.; Peters, S.; Gray, J. A.; Hunter, A. J. *Behav. Brain. Res.* **1999**, *99*, 81.
16. Bymaster, F. P.; Carter, P. A.; Peters, S. C.; Zhang, W.; Ward, J. S.; Mitch, C. H. *et al. Br. Research* **1998**, *795*, 179.
17. Moltzen, E. K.; Pedersen, H.; Bogeso, K. P.; Meier, E.; Frederiksen, K.; Sanchez, C.; Lembol, H. L. *J. Med. Chem.* **1994**, *37*, 4085.
18. Clark, M.; Cramer, R. D., III; Opdenbosch, N. V. *J. Comput. Chem*. **1989**, *10*, 982.
19. Dewar, M. J. S.; Zoebich, E. G.; Healy, E. F.; Stewart, J. J. P. *J. Am. Chem. Soc.* **1985**, *107*, 3902.
20. Schertler, G. F. K.; Villa, C.; Henderson, R. *Nature* **1993**, *362*, 770.
21. Weiner, S. J.; Kollman, P. A.; Case, D. A.; Singh, U. C. *J. Am. Chem. Soc.* **1984**, *106*, 765.
22. Luthy, R.; Bowie, J. U.; Eisenberg, D. *Nature* **1992**, *356*, 83.
23. Curtis, C. A. M.; Wheatley, M.; Bansal, S.; Birdsall, N. J. M.; Eveleigh, P.; Pedder, E. K.; Poyner, D.; Hulme, E. C. *J. Biol. Chem.* **1989**, *264*, 489.
24. Paquet, J. L.; Trumpp-Kallmeyer, S.; Hoflack, J.; Hibert, M.; Leppik, R. 1995, personal communication.
25. Wess, J., Blin, N.; Mutschler, E.; Bluml, K. *Life Sci.* **1995**, *56*, 915.
26. Reslé, S. *Pharmacochimie de la minaprine: synthèse d'analogues et de métabolites, approche vers le mécanisme moléculaire d'action*, Louis Pasteur University of Strasbourg, 1982, PhD Thesis.
27. Moureau, F. *Recherche d'un modèle de pharmacophore pour les ligands des récepteurs muscariniques de type M_1 par l'étude comparative de leurs relations structure-activité*, Notre Dame de la Paix University, Namur, 1988, PhD Thesis.
28. Serrano, L.; Bycroft, M.; Fersht, A. R. *J. Mol. Biol.* **1991**, *218*, 465.
29. Evrard, G.; Michel, A.; Durant, F. *Acta Crystallogr, Sect. A* **1981**, *37*, C70.
30. Michel, A.; Gustin, R.; Evrard, G.; Durant, F. *Bull. Soc. Chim. Belg.* **1982**, *91*, 123.
31. Van der Brempt, C.; Durant, F.; Norberg, B.; Evrard, G. *Acta cryst.* **1985**, *41*, 1532.
32. Trumpp-Kallmeyer, S.; Hoflack, J.; Bruinvels, A.; Hibert, M. *J. Med. Chem.* **1992**, *35*, 3448.
33. Wess, J.; Gdula, D.; Brann, M. R. *EMBO J.* **1991**, *10*, 3729.